

An estimating method of predicted seismic ground motions and an arrangement of remote monitoring seismographs for early detection of earthquake-damages

T.Takatani
Maizuru College of Technology, Kyoto, Japan

S.Takada & S.Fukui
Kobe University, Japan

T.Fuke
Osaka Gas Co., Ltd, Japan

ABSTRACT: It is very important to obtain various information of earthquake damages to lifeline systems as quickly and accurately as possible in order to make quick functional recovery for damaged lifeline facilities. This paper proposes a method to estimate seismic ground motions at arbitrary locations by using remote monitoring seismograph data observed at limited locations. In this proposed method the shape interpolating function is applied to the estimation method of seismic ground motions. In addition, a problem for making an effective arrangement of seismographs is discussed from the viewpoints of both spacing and installing locations of seismographs. The optimum spacing of seismographs is developed by minimizing the total costs of both equivalent costs to earthquake damages and installing costs of seismographs. The optimum installing locations of seismographs for a given spacing are evaluated by using a neural network system with a pattern recognition of earthquake damages to lifeline systems in recent urban earthquakes.

1 INTRODUCTION

It is well known that urban functions in highly developed modern cities are greatly dependent on lifeline systems such as electric power, gas, water, and communication network, and that the earthquake damages to those facilities cause urban functional disorder by which various activities in modern cities are seriously affected. The functional restoration of damaged lifeline facilities must be recovered as quickly as possible. It is indispensable, in the view of decision making of restoration strategies to damaged lifeline facilities, to obtain information of earthquake damages to lifeline systems as quickly and accurately as possible. Generally several seismographs are installed in the vicinity of important facilities of lifeline systems in order to obtain records for seismic ground motions which are closely related to the earthquake damages to lifeline systems.

Figure 1 shows a time flow for intra- and post-earthquake operations of lifeline systems under earthquake emergency. If the information of earthquake damages to lifeline systems can be obtained within one hour after the occurrence of an earthquake by an earthquake early detection system, and some emergency management of restoration works for lifeline systems can be accurately operated, the restoration works and functional recovery for lifeline systems may be smoothly and quickly performed. An effective arrangement of remote monitoring seismographs is necessary for the accurate estimation of seismic ground motions over an entire supply-region of lifeline systems, and for an accurate detection of

earthquake damages to lifeline systems as quickly as possible. This paper proposes an estimation method of seismic ground motions at arbitrary locations over an entire supply-region by using some remote monitoring seismograph data observed at limited locations in order to make quick and accurate activities for damage inspection within 100 minutes after an earthquake as shown in Figure

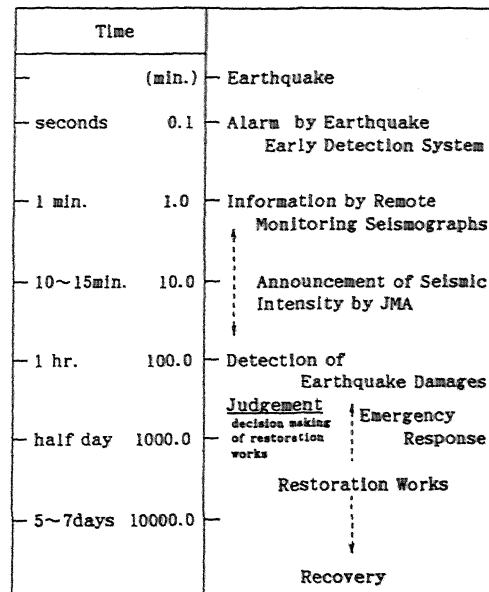


Figure 1. Time flow of intra- and post-earthquake emergency operations of lifeline systems.

1. The problem for making an effective arrangement of remote monitoring seismographs is discussed taking consideration of both spacing and installing locations of seismographs. The optimum spacing of seismographs can be evaluated for minimizing not only the disadvantage costs due to both earthquake damages and secondary disasters but also the cost of installing of seismographs from the viewpoints of damage inspection rate and detection rate. The optimum installing locations of seismographs under a given optimum spacing can be numerically evaluated by means of a neural network system whose learning data have various information as to earthquake damages of lifeline systems in recent urban earthquakes.

2. ESTIMATION OF SEISMIC GROUND MOTIONS

2.1 Outline of estimation method

The shape interpolating function (Washizu et al., 1981) used in FEM and/or BEM is applied to the estimating method of seismic ground motions at arbitrary locations by remote monitoring seismograph data observed at limited locations over an entire supply-region of lifeline systems. For the maximum acceleration values given at four points as shown in Figure 2, the maximum acceleration A_{max} at arbitrary location can be numerically evaluated from the following Equation (1) by using shape interpolating function.

$$A_{max} = \sum_{i=1}^4 N_i(\xi, \eta) A_i \quad (-1 \leq \xi \leq 1, -1 \leq \eta \leq 1) \quad \dots (1)$$

where, $N_1(\xi, \eta) = 0.25\xi\eta(1-\xi)(1-\eta)$,
 $N_2(\xi, \eta) = -0.25\xi\eta(1+\xi)(1-\eta)$,
 $N_3(\xi, \eta) = 0.25\xi\eta(1+\xi)(1+\eta)$,
 $N_4(\xi, \eta) = -0.25\xi\eta(1-\xi)(1+\eta)$

and, $A_i (i=1 \sim 4)$ is the maximum acceleration value observed at i -th location.

As the observation points rarely locate at the corners of square shape as shown in Figure 2, the estimating equation of acceleration value described above needs some modifications for an

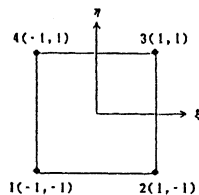


Figure 2. Observation points of acceleration

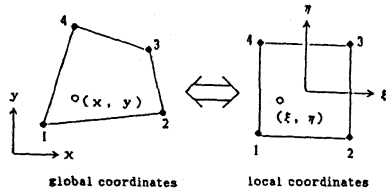


Figure 3. Global coordinates and local coordinates

arbitrary quadrangle shape.

If the observation points locate at the corners of arbitrary quadrangle shape as shown in global coordinates in Figure 3, the transformation from global coordinates to local coordinates in Figure 3 is required to evaluate acceleration value by Equation (1). Namely, if the location of (x, y) in global coordinates corresponds to the point (ξ, η) in local coordinates, the maximum acceleration value at the point (x, y) can be easily evaluated by Equation (1). The relationship between global and local coordinates can be represented by following equations.

$$x = \sum_{i=1}^4 N_i(\xi, \eta) x_i, \quad y = \sum_{i=1}^4 N_i(\xi, \eta) y_i \quad \dots \dots (2)$$

where, x_i and y_i are x and y coordinates of the i -th observation location, respectively.

The observed acceleration value can be significantly affected by the difference of ground conditions such as soft ground and hard one. The maximum acceleration value A_{max} at ground surface can be numerically obtained by multiplying the amplification factor A_m related with ground classification which is used in the attenuation equation (Kameda et al., 1980) of ground surface acceleration.

$$A_{max} = \sum_{i=1}^4 N_i(\xi, \eta) A_i \times \frac{A_m}{A_{m_i}} \quad \dots \dots (3)$$

where, A_{m_i} is an amplification factor of the i -th observation point.

2.2 Estimation results of seismic ground motions

Numerical examples for making estimation of seismic ground motions are illustrated in this section, and the maximum acceleration values at ground surface observed at 8 points located in a certain district are used in the estimation method of seismic ground motions. If the records of seismograph data can not be obtained, by assuming the epicenter and magnitude of earthquake the acceleration values at 8 points can be easily estimated from the following attenuation equation.

$$\left. \begin{aligned} A_0 &= \frac{111 \times 10^{0.534M}}{(\Delta + 30)^{1.856}} \quad (\Delta \geq \Delta_0(M)) \\ A_0 &= 99.6 \times 10^{0.0804M} \quad (\Delta < \Delta_0(M)) \\ \Delta_0(M) &= 1.06 \times 10^{0.242M} - 30 \end{aligned} \right\} \quad \dots \dots (4)$$

where, A_0 is a maximum acceleration value at base rock, Δ is an epicentral distance (km), and M is a magnitude.

The maximum acceleration value at ground surface can be estimated by multiplying the amplification factor. Seismic intensity distribution in the entire supply-region of lifeline systems can be evaluated from the estimation method of seismic ground motions described above.

Figures 4 and 5 show seismic intensity distributions estimated from acceleration values at 8 points evaluated by Equation (4) for near field earthquake and for far field one, respectively. Seismic intensity distribution for near

field earthquake in Figure 4 shows that the seismic intensity only in the region close by epicenter is in level VII, and that the seismic intensity on other regions is in level VI. Seismic intensity distribution for far field earthquake in Figure 5 shows that the seismic intensity of almost estimating regions is in level V because an epicenter of this earthquake is far from the estimating region.

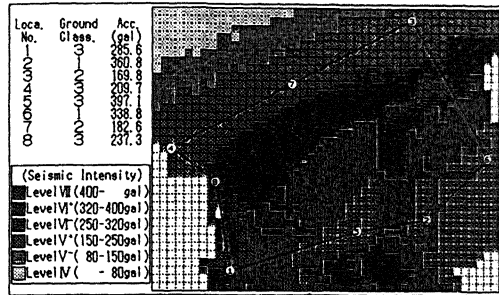


Figure 4. Estimation results of seismic intensity for near field earthquake

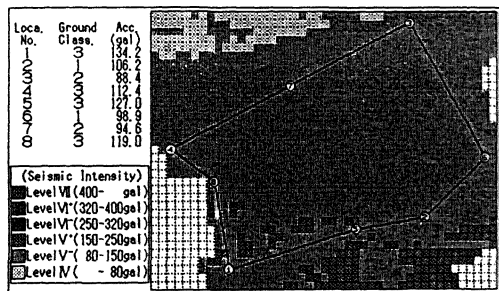


Figure 5. Estimation results of seismic intensity for far field earthquake

3 OPTIMUM ARRANGEMENT OF SEISMOGRAPHS

Five major factors to give an effective arrangement of remote monitoring seismographs for the early detection of earthquake damages to lifeline systems, are considered as follows:

- Region where severe damage is expected (soft ground and liquefaction area)
- Regions with high potential of outbreak of second disaster (high population density, high density of buried pipeline network and important facilities)
- Region where seismic disaster had ever suffered, and Regions with high potential of seismic sources and active faults
- Arrangements of a restoration block for lifeline system (an area divided for early recovery workings)
- Economic effects for the installing of seismic monitoring system (optimum spacing and installing locations of seismographs under economic constraints)

In this paper, the optimum spacing of seismographs is developed under economic constraints.

3.1 Definition of an objective function for optimum spacing of seismographs

Two major terms for an objective function for optimum spacing seismographs are considered in this paper. One is a cost of installing of seismographs, and the other is a total cost including the disadvantage costs due to second disaster, emergency supply halt, and damage inspections for lifeline systems. The former increases as the installing spacing of seismographs while the latter decreases. The definition of an objective function for optimum spacing of seismographs is to minimize total costs of both equivalent to earthquake damage and installing costs of seismographs.

The following inspection and detection rates associated with information given by seismographs are used in this paper.

$$\text{Inspection Rate } Q = \frac{\text{Area of inspection-finished region}}{\text{Area of inspection region}}$$

Number of damages confirmed by field survey which has priority

$$\text{Detection Rate } P = \frac{\text{Number of damages confirmed by field survey which has priority decided by seismograph data}}{\text{Total number of damages}} \quad \dots (5)$$

where, the numerator of inspection rate Q means an area whose damage state is confirmed by investigators dispatched depending the information of seismograph data after the occurrence of an earthquake.

The inspection rate increases as the number of investigators and the progress of damage inspection activities. For the case that needs quick judgement of the supply-stop in order to prevent lifeline systems from the outbreak of second disaster, the inspection rate can be decided in response to the mobilization system for investigation. Namely, if the damage state to lifeline systems can be estimated to some degree at the initial stage of field inspection, it is evident that the detection rate approaches to 100% at the initial stage of field inspection, and that the probability of outbreak of second disaster decreases rapidly. Accordingly, it can be expected that the detection rate of earthquake damages increases rapidly by the information of effective seismograph data under same inspection rate. The inspection rate Q and detection rate P can be assumed to be increasing functions in progress for recovery workings. The relation among the spacing of seismograph R and these rates can be represented by the following equation.

$$P = Q(1-Q) \alpha R \quad \dots (6)$$

where, α is a coefficient depending on P and Q values.

Figure 6 shows a relationship between the inspection rate Q and detection rate P for a R parameter shown in Equation (6). As is obvious from this figure, in case of a R=0.2 even if damage inspection rate Q is small, damage detection rate P becomes large. On the other hand, in case of a R=10.0 damage detection rate P does not increase easily even if damage inspection rate Q is large.

Next, the following two terms which are close

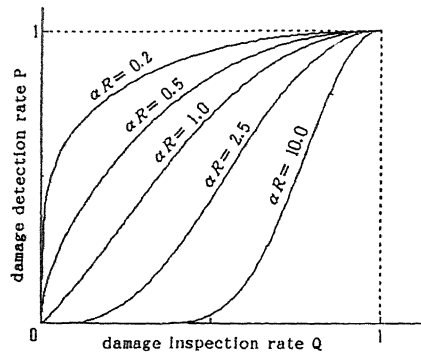


Figure 6. Efficiency diagram of damage detection activity

ly related to the second disaster by earthquake damages are introduced. Then the relationship among the detection rate P and these terms are investigated.

- ① second disasters which could not be avoided after direct damages to lifeline systems
- ② service drop to customers caused by the fact that supply could not be accurately stopped.

where, the rate of outbreak of second disaster E and the rate of disadvantage T for customers due to supply-stop are defined as follows.

$$\text{Rate of second disaster } E = \frac{\text{Number of second disaster outbreak}}{\text{Total number of damaged main pipe}} \quad \dots (7)$$

$$\text{Rate of disadvantage } T = \frac{\text{Number of customers suffered supply-stop}}{\text{Total number of customers}}$$

The rate of outbreak of second disaster E and the rate of disadvantage T are considered to be reasonable to assume that these are proportional to seismic ground motions. Then these rates which are closely related to the detection rate P can be represented by following equations.

$$E = C_1 e^{-\beta_1 P}, \quad T = C_2 e^{-\beta_2 P} \quad \dots (8)$$

where, $C_i (i=1,2)$ are the coefficients for the outbreak of second disaster at detection rate $P=0$, and $\beta_i (i=1,2)$ are the decreasing ratios for the rate of outbreak of second disaster E and the rate of disadvantage T.

Then, the disadvantage costs caused by the second disaster and supply-stop are assumed to be following terms under the condition of detection rate $P=0$.

- ① The disadvantage cost due to outbreak of second disaster \dots A Yen
- ② The cost due to disadvantages to customers in supply-stop \dots B Yen

Concerning ①, second disaster is assumed to break out at main pipeline whose supply is large in quantity, while with respect to ② service drop is assumed to occur at branch pipelines. The disadvantage costs A and B, which depend on either

the materials and states of damaged pipeline or the seismic intensity, can be represented by following equations.

$$\begin{aligned} A &= q_1 \cdot \pi R^2 = a \cdot k_1 \cdot l_1 \cdot \pi R^2 \\ B &= q_2 \cdot \pi R^2 = b \cdot k_2 \cdot l_2 \cdot \pi R^2 \end{aligned} \quad \dots (9)$$

where, k_i : damage ratio (number/km) per 1km pipeline length depending on the materials of pipeline or the seismic intensity
 l_i : average construction length (km/km²) of main and branch pipeline per 1km²
 a : disadvantage cost (Yen/number) due to second disaster occurred by damages at main pipelines
 b : disadvantage cost (Yen/number) due to troubles at supply stop region caused by damages at branch pipelines

Consequently, the objective function becomes the sum Z consisted of various costs such as construction of seismographs, disadvantage costs represented by Equation (9), and costs required for making up the level of the detection rate P, which is assumed to be proportional to the value of P. That can be represented by the following equation.

$$Z = \frac{S}{\pi R^2} n + (q_1 C_1 e^{-\beta_1 P} + q_2 C_2 e^{-\beta_2 P} + q_3 P) \pi R^2 \quad \dots (10)$$

where, S is service area (km²), n is a cost to be necessary for construction of a seismograph, q_3 is a total cost such as personnel expenses and machine parts expenses required for the detection rate P per 1km² to become 1.0.

At first, if the goal of detection rate P at some inspection rate Q_1 is assumed to be P_1 , there are an infinite number of (α, R) combination which satisfies Equation (6) for P_1 and Q_1 . In case of $Q=Q_1$ and $\alpha = \alpha_1$, R_2 which minimizes the objective function Z can be obtained from Equation (10) for an arbitrary combination (α_1, R_1) . At this time, if R_2 does not equal to R_1 , R which equals to R_1 is carefully searched for a different value α_1 . If R_2 equals to R_1 , $R=R_2=R_1$ satisfies both Equation (6) and (10) and becomes an optimum spacing of seismographs which satisfies the assumed detection rate and desired economic effect.

3.2 Numerical example

As a numerical example, the following data are used in this paper.

$$\begin{aligned} C_1 &= 0.3, \quad C_2 = 0.5, \quad a = 1000, \quad b = 100, \quad l_1 = 1.0, \quad l_2 = 4.0, \\ q_3 &= 1000, \quad \beta_1 = 3.4, \quad \beta_2 = 3.9, \quad n = 1000, \quad S = 10000, \\ k_1 &= 0.0, \quad k_2 = 1.0 \text{ for } 100\text{gal}, \\ k_1 &= 1.5, \quad k_2 = 3.5 \text{ for } 300\text{gal} \end{aligned}$$

Optimum spacing of seismographs is numerically evaluated for inspection rate $Q=20\%$ as shown in Figure 7. The values of k_1 and k_2 are damage ratios of main and branch pipelines for both ground acceleration values 100gal and 300gal. This figure shows that the optimum spacing of seismographs for 100 gal reaches a constant as damage detection rate P increases, and that the

optimum spacing for 300gal does not increase any more even if the detection rate P increases and becomes almost of constant value for detection rate P in comparison with that for 100gal. For this reason, it can be considered that the relation between the inspection rate Q and detection rate P would be a linear relationship for the case of severe damages to lifeline systems by strong seismic ground motion.

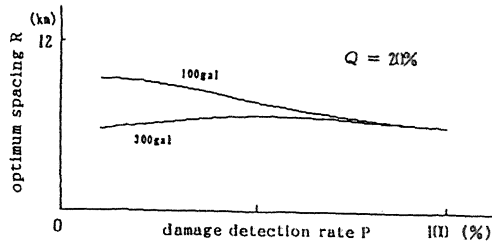


Figure 7. Optimum spacing of seismographs in case of damage inspection rate Q=20%

3.3 Optimum installing location of seismographs

A neural network system (Rumelhart et al., 1986) is introduced to obtain optimum installing locations of seismographs in this paper. The learning procedure of the neural network is called 'back-propagation' for networks of neurone-like units. This learning procedure repeatedly adjusts the weights of the connections in the network so as to minimizing a measure of the difference between the actual output vector of the net and the desired output vector. In this

Table 1. Earthquake list used as learning data of neural network system

Name of Earthquake	Period	Longitude	Latitude	M
Tozan Earthquake in China	1976	116° 36' /E	36° 54' /N	7.8
Miyagiken-oki Earthquake	1978	142° 17' /E	38° 15' /N	7.4
Jihonkai-chubu Earthquake	1983	139° 08' /E	40° 36' /N	7.7
Chibaken-tohooki Earthquake	1987	140° 29' /E	35° 21' /N	6.7

paper the information of earthquake damages to gas and water pipelines in recent urban earthquakes in Table 1 is used as learning data of the neural network system. The learning data generally consists of input and output data. The input data in each damaged area including seismic intensity, ground classification, active faults, important pipeline facilities, pipeline density and strength of pipeline joint are used for neural network system, while the information of earthquake damage states such as severe, medium, slight and no damage is used as output data of the neural network.

The learning of neural network is to find a set of weights which ensure that for each input vector an actual output vector produced by the network is sufficiently close to the desired output vector. Total error can be evaluated by comparing the actual and desired output vectors for every learning case. In this paper the total error E is defined as follows.

$$E = \frac{1}{N} \sum_i \sum_j (y_{ij} - d_{ij})^2 \quad \dots (11)$$

where i is an index over input-output pairs, j is an index over output units, y is the actual state of the output unit, d is its desired state, and N is number of learning data. In back propagation method it is, in general, necessary to numerically evaluate the partial derivative of total error E with respect to each weight in the network system in order to minimize E by gradient descent.

The neural network system consists of three layers and input layer has 20 units, hidden one is 40 units, and output one is 4 units. The number of learning data is 590 and that of repetitions is 150,000. This neural network system whose learning has already finished for input-output pairs of past earthquake damages to pipelines are applied to a problem of installing locations of seismographs. It is necessary to investigate this neural network system for 14 standard pattern recognition data of earthquake damages to lifeline systems in Table 2 before using this system.

The characteristics of earthquake damages for each earthquake in Table 1 can be represented by

Table 2. Recognition data for learning result of neural network system

Input factors	Ground Classification			Geographical Features			Region where geological state changes suddenly		Active Faults		Density of Pipeline Network			Strength of Pipeline Joint			Seismic Intensity				
	I	II	III	A	B	C	Exist	No	Exist	No	High	Medium	Low	Strong	Medium	Weak	IV	V	V	VI	
1. Standard																					
2. I (Hard)																					
3. III (Soft)																					
Potential of Liquefaction																					
4. High																					
5. Low																					
6. Region where geological state changes suddenly																					
7. Active Faults																					
Density of Pipeline Network																					
8. High																					
9. Low																					
Strength of Pipeline Joint																					
10. Strong																					
11. Weak																					
Seismic Intensity																					
12. IV (~ 80gal)																					
13. V (80~150gal)																					
14. VI (250~400gal)																					

multiplying an appropriate weight to the output vector of this system whose 4 neuron-like units have four damage grades such as severe, medium, slight and no damage. Figure 8 shows output results of this neural network system for earthquakes in Table 1 by multiplying the following weight to each damage grade of the output vector.

$$\text{Output value} = (\text{severe damage}) + (\text{medium damage}) * 0.7 + (\text{slight damage}) * 0.3 \dots (12)$$

This figure indicates that the factors such as high potential of liquefaction, existing of faults, weak pipe material and high seismic intensity are closely related with pipe damages.

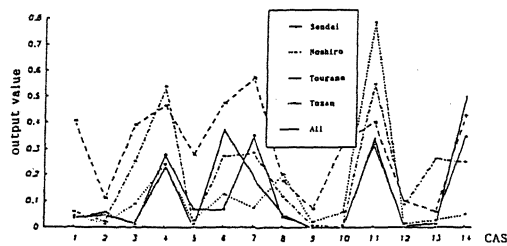


Figure 8. Effects of weight of each factor to the learning results of neural network system

Next, the results of the neural network system described above are applied to a practical problem. We divide gas supply-regions in Osaka area into small meshes as $382m \times 308m$ which have a weight including various information of each input datum in learning data of the neural network described above. In doing so, the seismic intensity grade for each mesh is analytically evaluated for a presumed earthquake with given location and magnitude. The neural network system can estimate the grade of earthquake damages to lifeline systems.

Figure 9 shows a weight distribution for each mesh and locations of telemeter stations which are illustrated in dot marks in Osaka area. The locations of telemeter stations are chosen as a subject to the installing locations of seismographs. The priority for installing locations of seismographs can be in order by the weight summation of meshes within the region bounded by a circle whose center and radius are the location of telemeter station and a given spacing of seismo-

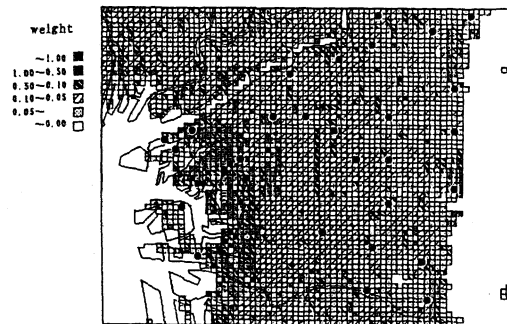


Figure 9. Weight distribution and locations of telemeter stations

graphs, respectively.

Figure 10 illustrates resultant order for installing locations of seismographs for the case of optimum spacing $R=4km$. It is evident from this numerical example that the effective installing locations and order of seismographs can be numerically evaluated by the neural network system whose learning data have various information of damaged lifeline systems.

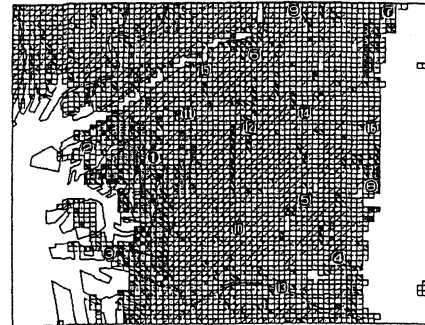


Figure 10. Resultant order for installing locations of seismographs (optimum spacing $R=4km$)

4 CONCLUSIONS

An estimating method of seismic ground motions in an entire supply-region by the remote monitoring seismograph data observed at limited locations was proposed in this paper. It was, moreover, evident that the optimum spacing can be evaluated by minimizing an objective function under economic constraints, and also that the optimum installing locations and the order of seismographs can be numerically evaluated by using the neural network system whose learning data have various information of earthquake damages to lifeline systems in recent urban earthquakes.

Although the estimation method of seismic ground motions, the effective arrangement of seismographs and the application of a neural network system to installing locations and order of seismographs are based on many preliminary assumptions in this paper, it is hoped that this type of work herein may be fruitfully extended to the regional seismic monitoring systems.

REFERENCES

- 1) Washizu, H., Miyamoto H., Yamada Y., Yamamoto Y., & Kawai T. 1981. Handbook of Finite Element Method I, Baihukan (In Japanese).
- 2) Kameda H., Sugito M., & Asamura, T. 1980. Simulated Earthquake Motions Scaled for Magnitude, Distance, and Local Soil Conditions. Proc. 7WCEE. 2: 295-302.
- 3) Rumelhart, D.E., McClelland, J.L. & PDP Research Group 1986. Parallel Distributed Processing. Vol. 1 & 2, MIT Press, Cambridge.